Using Mathematics to Find the Imperfections in Images of Materials

Amel Ahamseldeen Ali Alhassan,
Supervisors:
Prof. Dr. Benjamin Berkels (RWTH Aachen)
Prof. Dr. Knut Müller-Caspary (Research Center Jülich)
Mr. Hoel Robert (Research Center Jülich)
Dr. Tevfik Onur Mentes (Elettra)

RWTH Aachen

28 September 2021

Biography


Estonia
Latvia
Lithuania
Belarus
Poland
Moscow
Москва
Kazakhstan
China
North Sea
United Kingdom
Netherlands
Berlin
Warsaw
Kyiv
Київ
Ukraine
Kyrgyzstan
Uzbekistan
Tajikistan
Czechia
Slovakia
Moldova
Austria
Hungary
France
Turkmenistan
Bhutan
Nepal
Black Sea
Azerbaijan
Afghanistan
Portugal
Madrid
Spain
Italy
Tyrrhenian Sea
Greece
Ankara
Istanbul
Turkey
Pakistan
India
Iran
Syria
Iraq
Lebanon
Mediterranean Sea
Tunisia
Israel
Jordan
Morocco
Persian Gulf
United Arab Emirates
Cairo
القاهرة
Riyadh
الرياض
Mumbai
Bengaluru
Algeria
Egypt
Saudi Arabia
Oman
Western Sahara
Libya
Jeddah
جدة
Red Sea
Arabian Sea
Mauritania
Yemen
Dakar
Senegal
Mali
Niger
Sudan
Gulf of Aden
Gambia
Djibouti
Chad
Guinea
Burkina Faso
Sierra Leone
Benin
Nigeria
South Sudan
Somalia
Côte d'Ivoire
Liberia
Togo
Ghana
Abidjan
Lagos
Central African Republic
Cameroon
Uganda
Kenya
Nairobi
Equatorial Guinea
Google
Layers
Map data ©2021 Google, INEGI, SK telecom
Germany
Terms
Privacy
Send feedback

AMEL ALHASSAN

MATHEMATICIAN AND PHYSICIST

Amel Shamseldeen Ali Alhassan

Research assistant, Aachen Institute for Computational Engineering Sciences (AICES), RWTH Aachen, Germany (February 2021- present)

ICTP Postgraduate diploma, condensed matter, Adus-Salam International Center for Theoretical Physics , Italy (September 2020)

Mathematics and Physics lecturer, Nile University, Sudan (2013- present)

MSc. Mathematical Sciences, African Institute of Mathematical Sciences and Kwame Nkrumah University of science and Technology, Ghana (June 2013)

BSc. with honor degree Science – Physics: University of Khartoum, Sudan (September 2010)

CV

Table of Contents

The evolution of imaging process

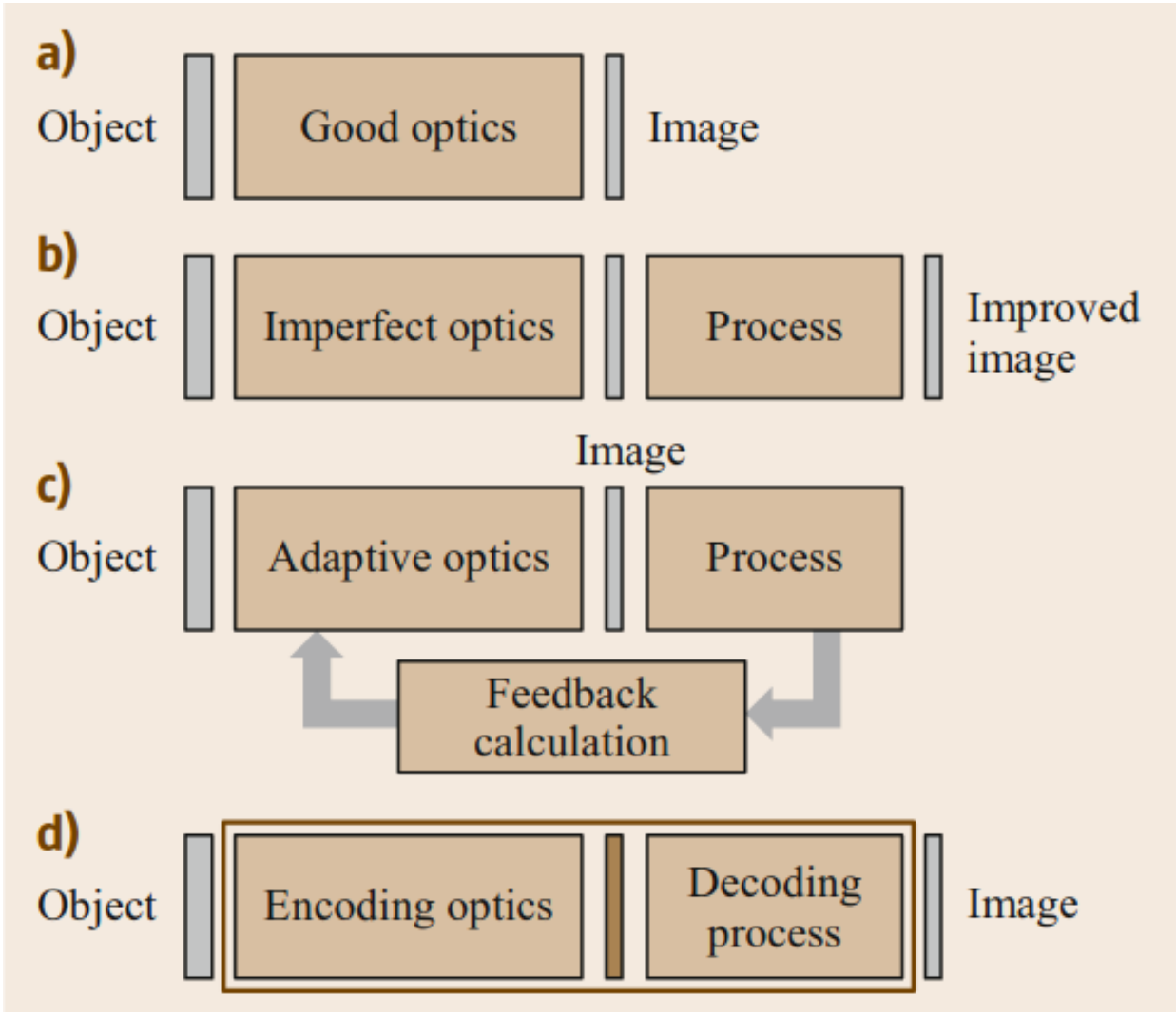

John Rodenburg and Andrew Maiden, Ptychography, Springer Handbook of Microscopy- ch17 Pthychography, 2019, doi: 978-3-030-00069-1_17

Imaging with CTEM and STEM

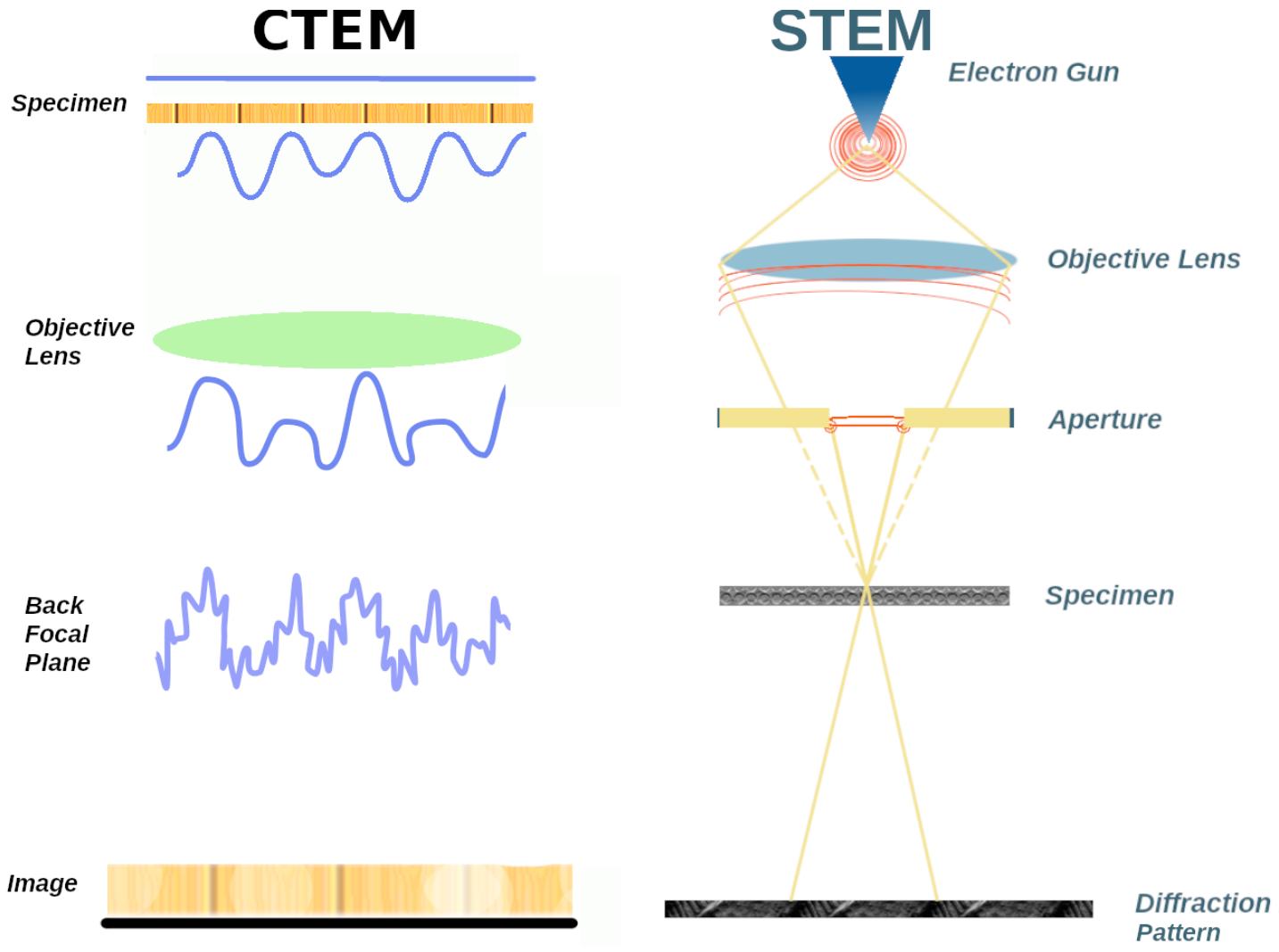

Layout

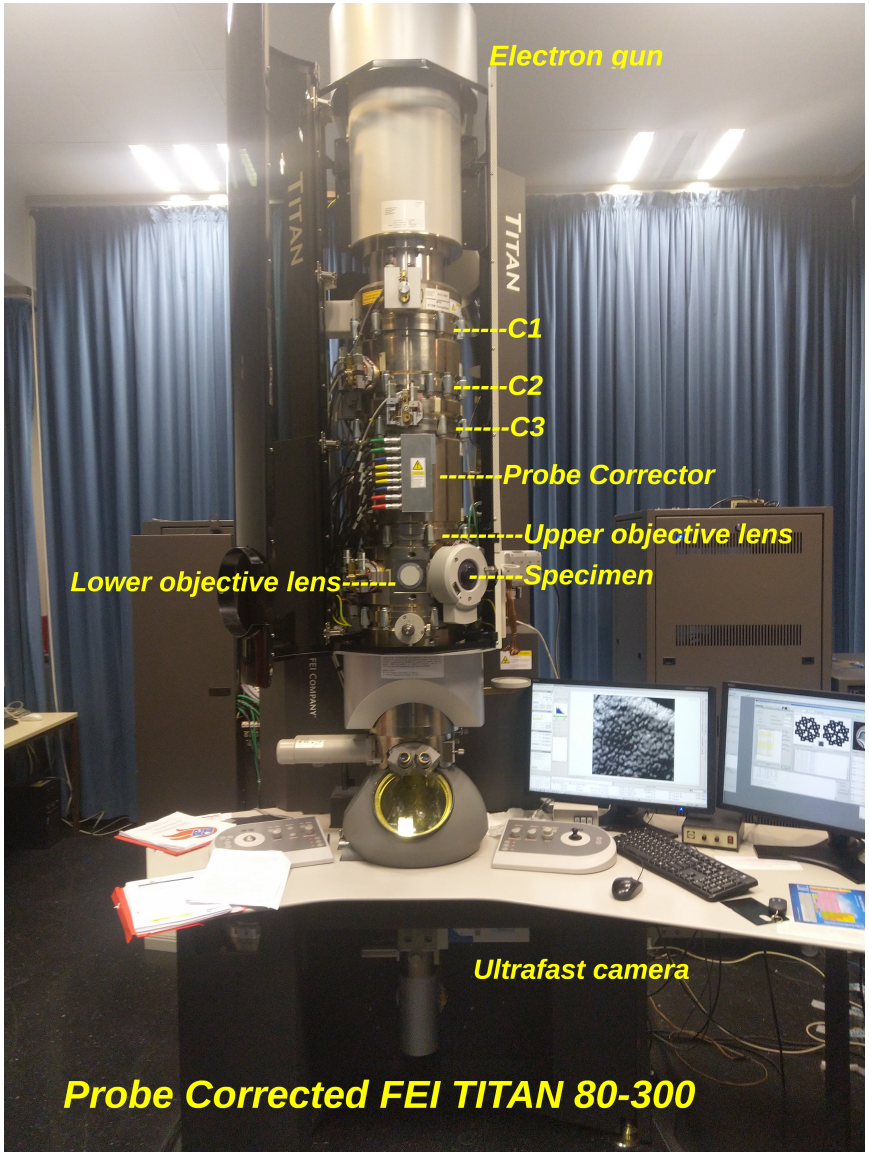

H. L. Robert

Information at the Detector level of STEM

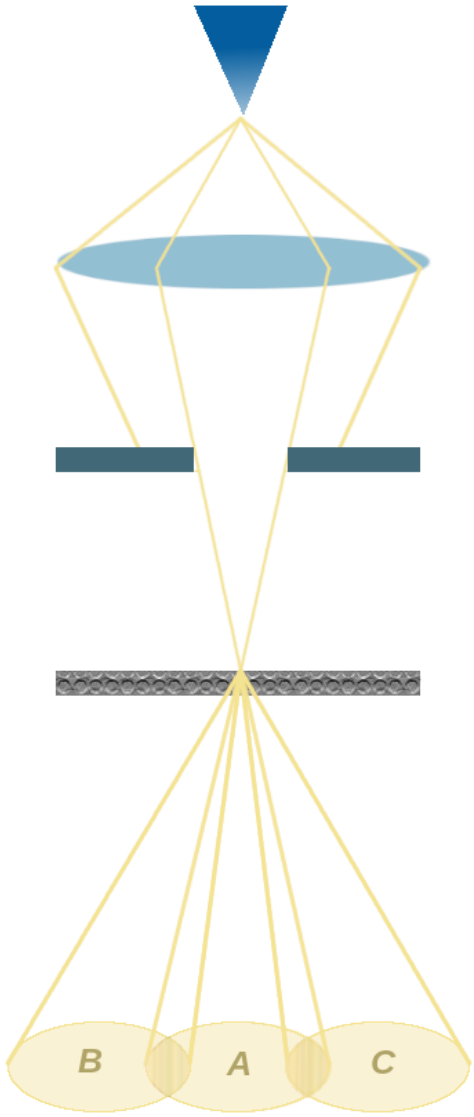

- The intensity is recorded, therefore the phase of the diffraction pattern is lost.
- The overlap between the diffracted discs gives information about the relative phase.
- Rastering the illumination over the specimen allows the retrieval of the unique value of the phase space of the diffraction pattern.

Momentum Resolved (4D) STEM

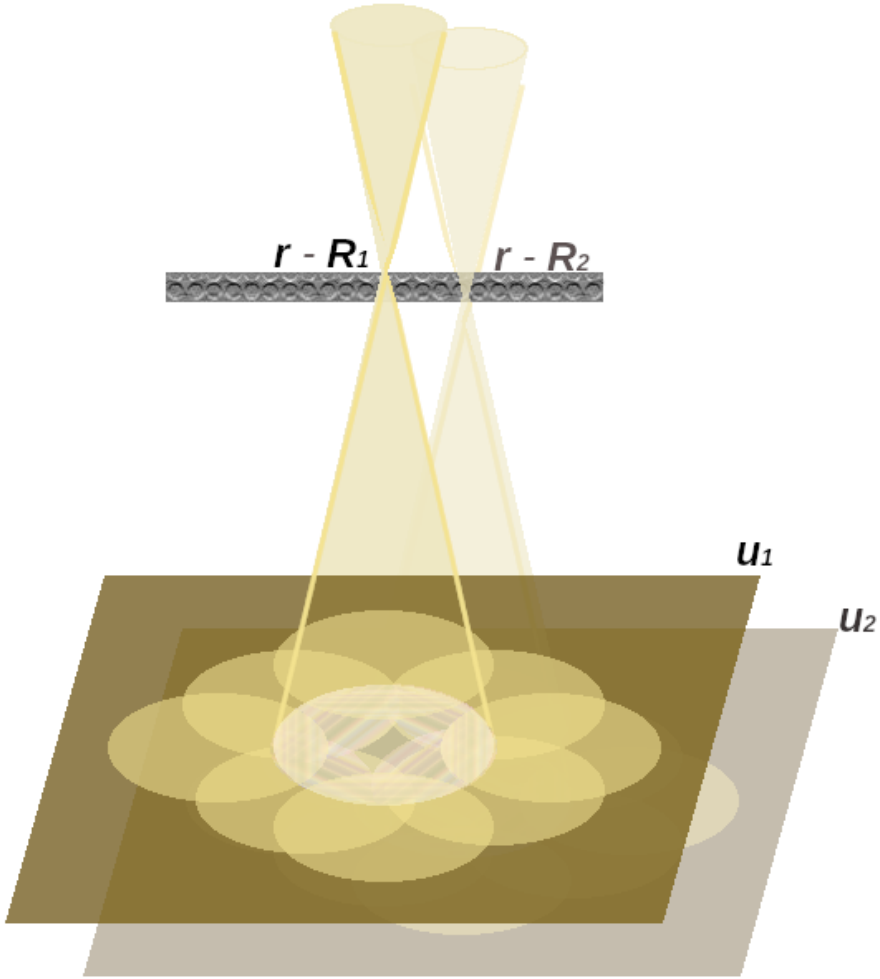

Figure: Momentum resolved STEM Imaging

- probe raster across the specimen.
- 2D scan positions in real space.
- 2D diffraction patterns in momentum space.

Conventional Imaging Modes

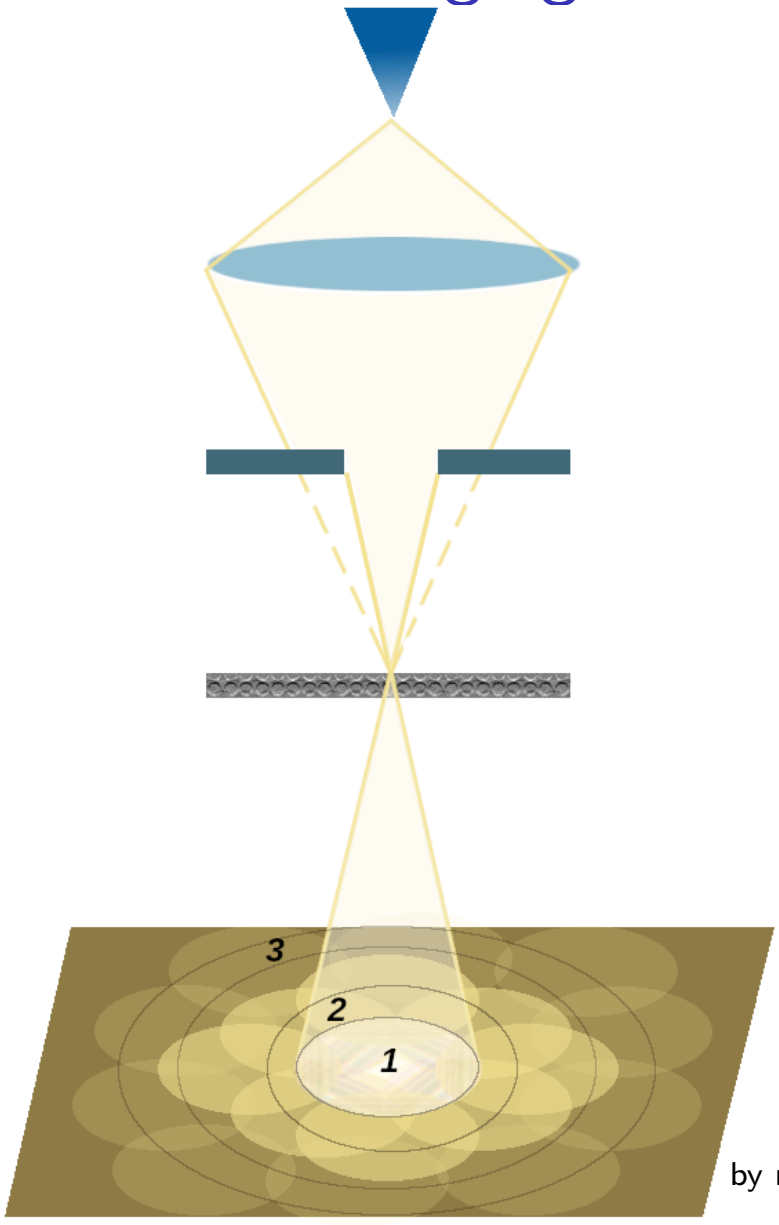

1- Bright Field

primary beam

2- Annular Bright Field

weakly scattered electrons.
low Z atoms

3- Annular Dark Field

scattered electrons.
Z-contrast

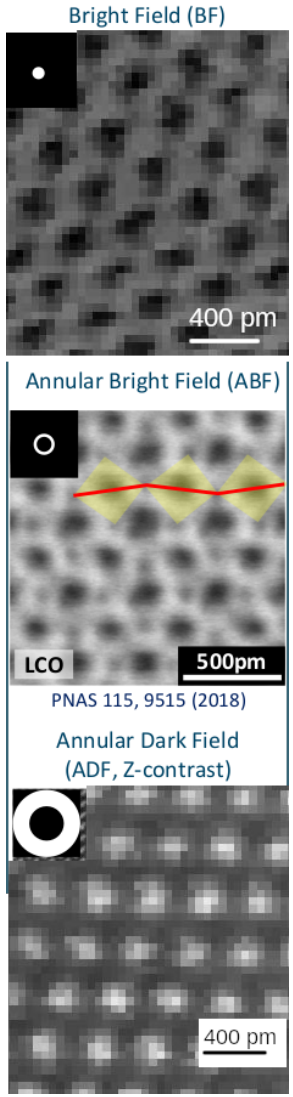

Z. Liao et. al., Metal–insulator-transition engineering by modulation tilt-control in perovskite nickelates for room temperature optical switching, PNAS, 2018

Nellist P. D.Scanning Transmission Electron Microscopy, Springer International Publishing, Cham, 2019

Stephen J. Pennycook and Peter D. Nellist, Scanning Transmission Electron Microscopy Imaging and Analysis,

4D data-set (used for ptychography)

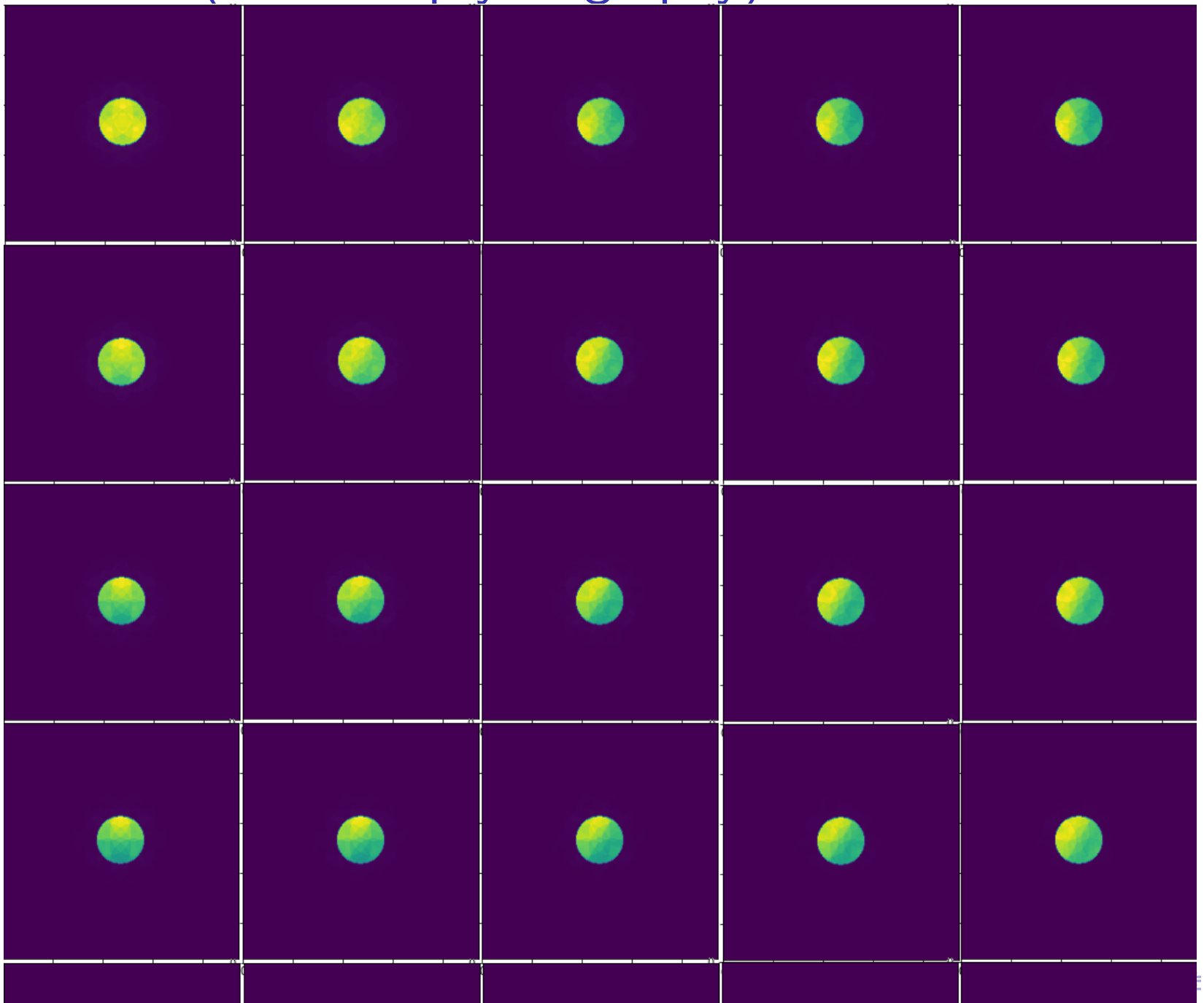

Ptychography vs other imaging techniques

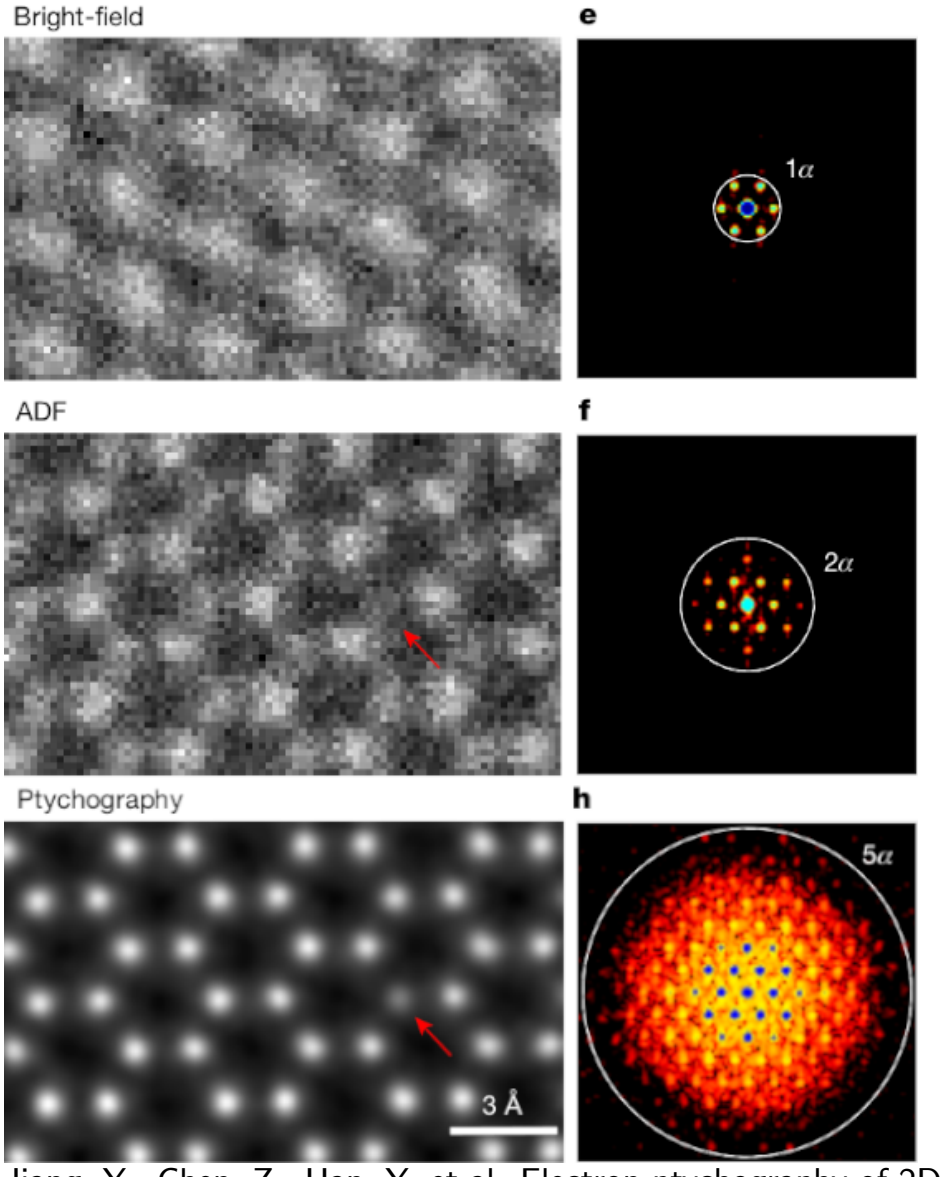

Monolayer MoS_2

- Coherent bright-field image,
- Incoherent ADF image,
- Ptychography

Sulfur monovacancy detectable in Ptychography

Ptychography

Super Resolution
High Contrast

Jiang, Y., Chen, Z., Han, Y. et al. Electron ptychography of 2D materials to deep sub-angström resolution. Nature 559, 343–349 (2018). https://doi.org/10.1038/s41586-018-0298-5

Lens Aberrations

$$\Phi(u) = \frac{2\pi}{\lambda}\left(\frac{1}{4}C_s(\lambda u)^4 - \frac{1}{2}C_1(\lambda u)^2 + \ldots\right)$$

$C_s \equiv$ spherical aberration, $C_1 \equiv$ defocus, $A_1 \equiv$ 2-fold astigmatism, $A_2 \equiv$ 3-fold astigmatism, $B_2 \equiv$ Coma.

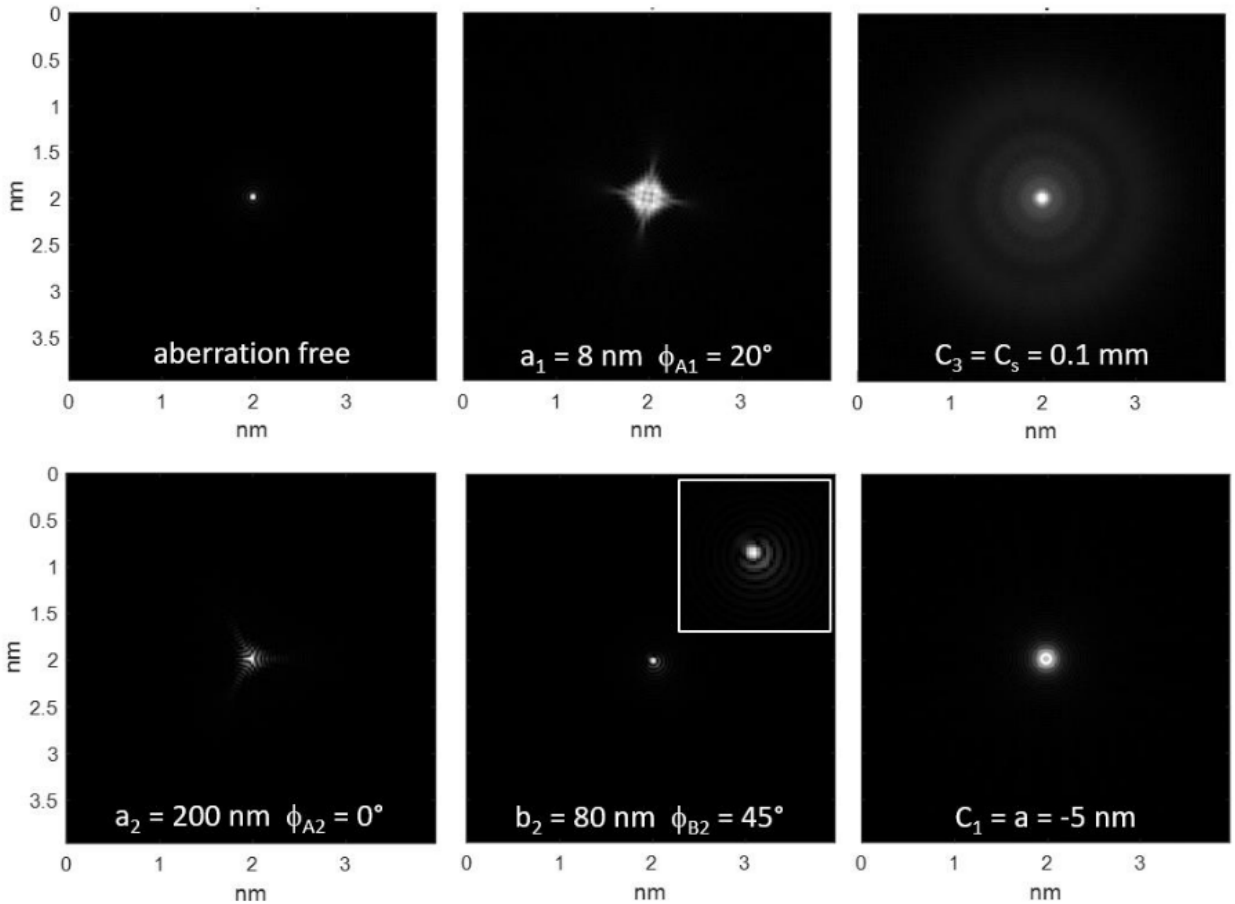

Imaging

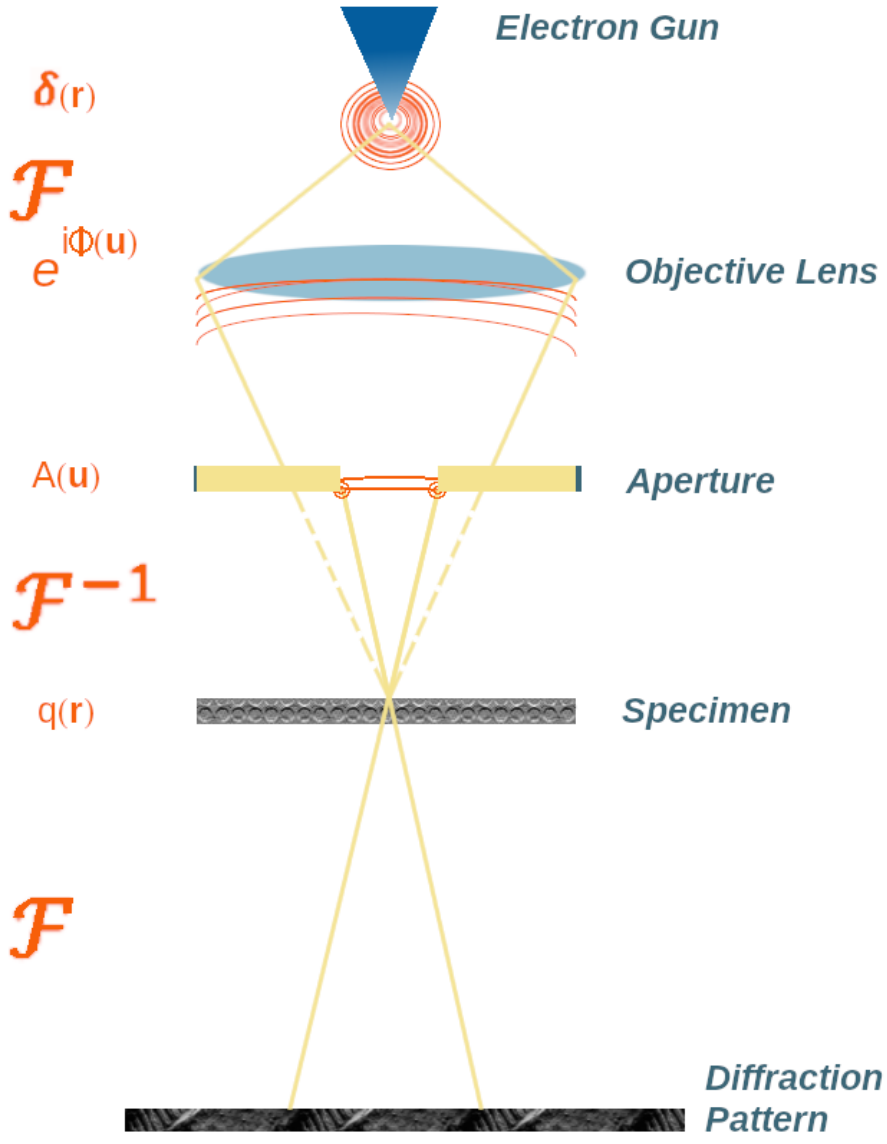
Electron Gun
δ(r)
ℱ
e^{iΦ(u)}
Objective Lens
A(u)
Aperture
ℱ⁻¹
q(r)
Specimen
ℱ
Diffraction Pattern

Important Formulae

The wave function after exiting the specimen

$$\psi(\vec{r}) = a(\vec{r} - \vec{R}).q(\vec{r}),$$

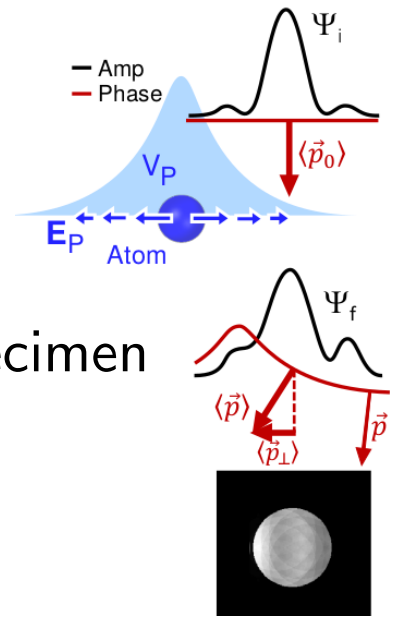

- a is the illumination
- q is the object transfer function (OTF) of the specimen

At the detector, the diffraction pattern is

$$M(\vec{u}) = \mathcal{F}[\psi(\vec{r})] = \int \psi(\vec{r}) e^{2\pi i \vec{u}\vec{r}} d\vec{r}.$$

J. Rodenburg and R. Bates, The theory of super-resolutionelectron microscopy via wigner-distribution deconvolution, Nat. Comm. 1992

John Rodenburg and Andrew Maiden,Ptychography, pages 819 –904. Springer International Publishing, 2019

Direct-ptychograohy algorithms

Steps of the ptychographic reconstruction methods

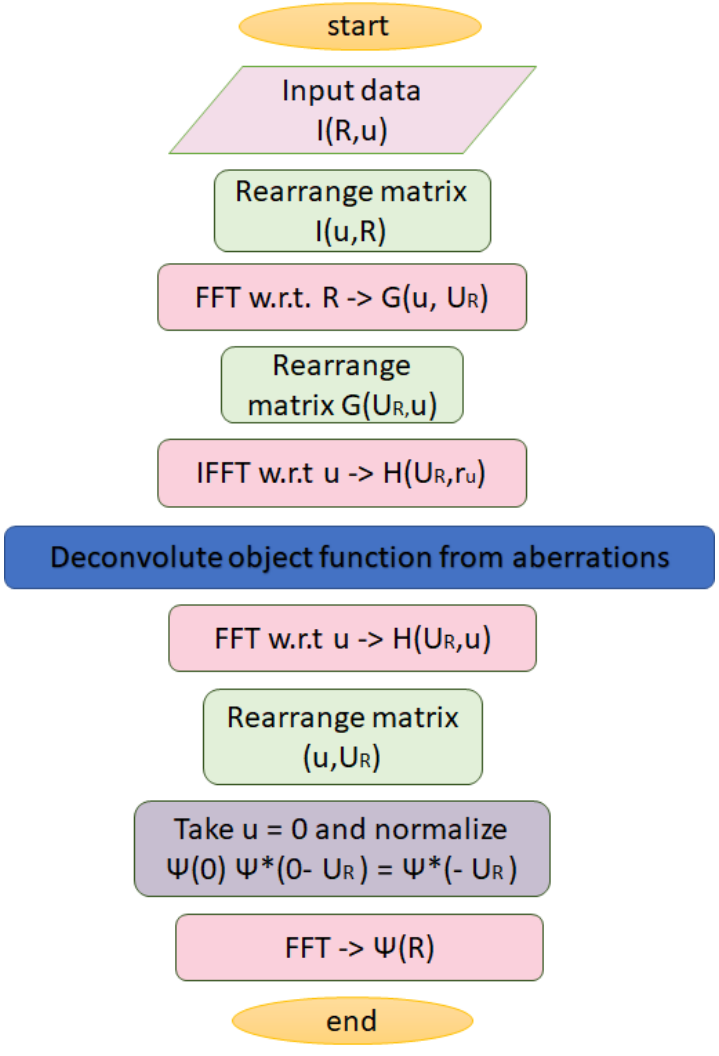

Full WDD

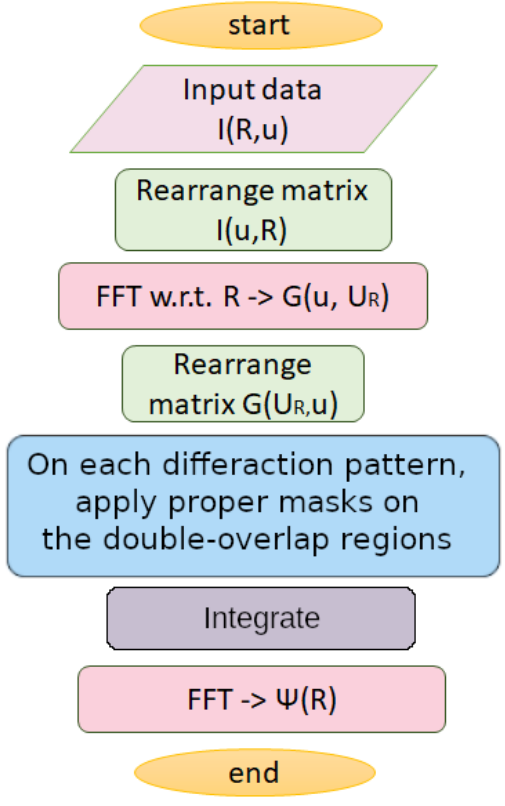

SSB: WDD under weak phase approximation

Iterative Ptychography

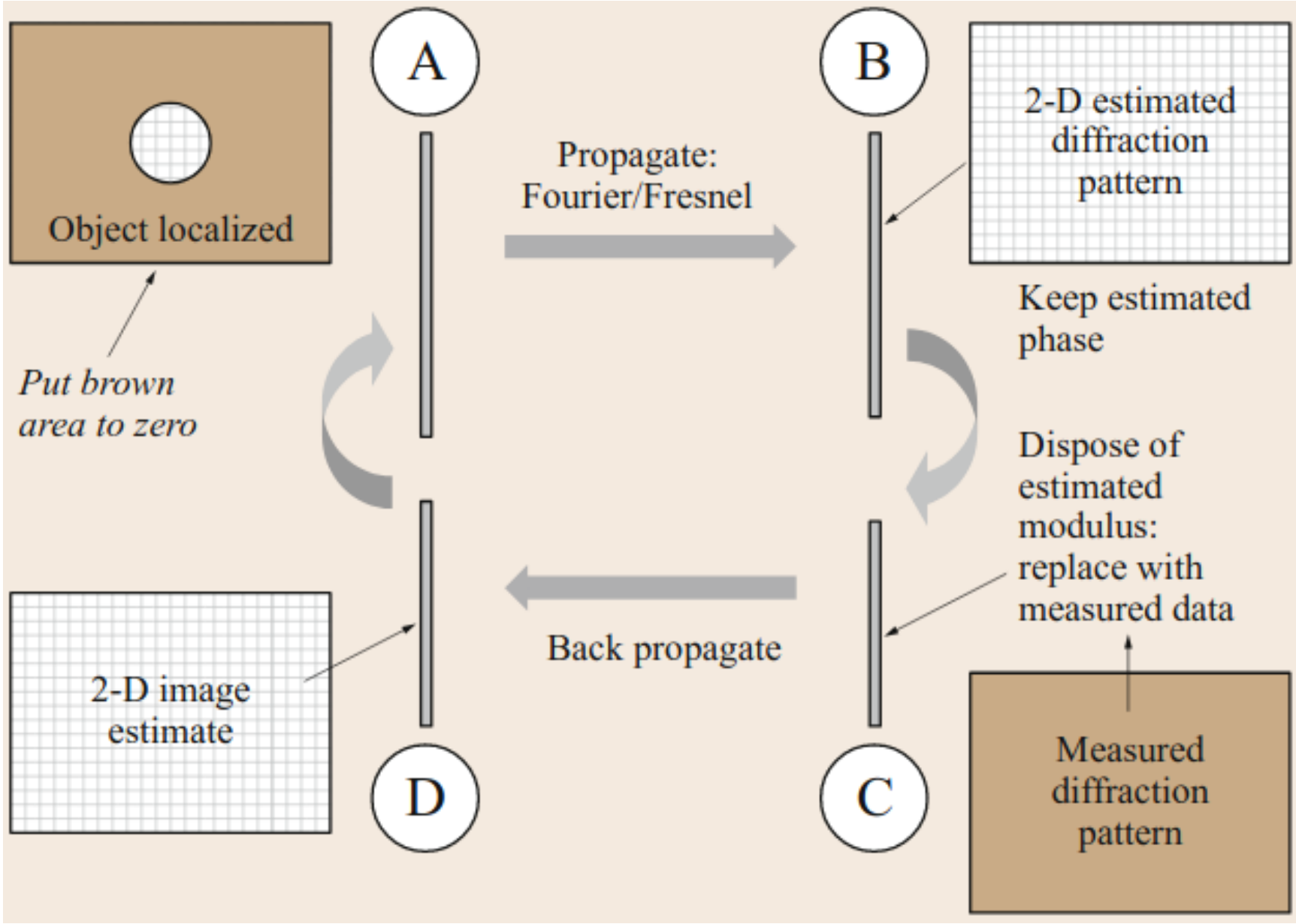

John Rodenburg and Andrew Maiden, Ptychography, Springer Handbook of Microscopy- ch17 Pthychography, 2019

ePIE Algorithm

$$\psi = aq$$

waiting of the

$$q_{NEW} = q + \frac{|a|^2}{|a_{max}|^2}(\psi_{NEW} - \psi_e)$$

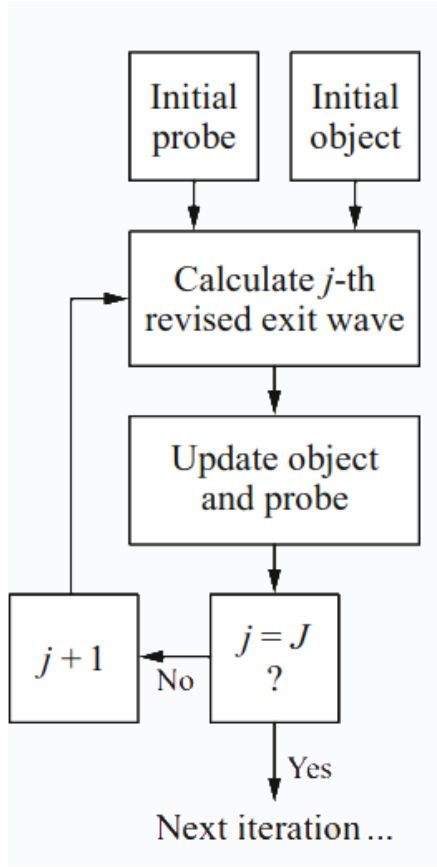

A.M. Maiden, J.M. Rodenburg: An improved ptychographical phase retrieval algorithm for diffractive imaging, Ultramicroscopy, 2009
John Rodenburg and Andrew Maiden, Ptychography, Springer Handbook of Microscopy- ch17 Pthychography, 2019

Resilience to Corrupt data

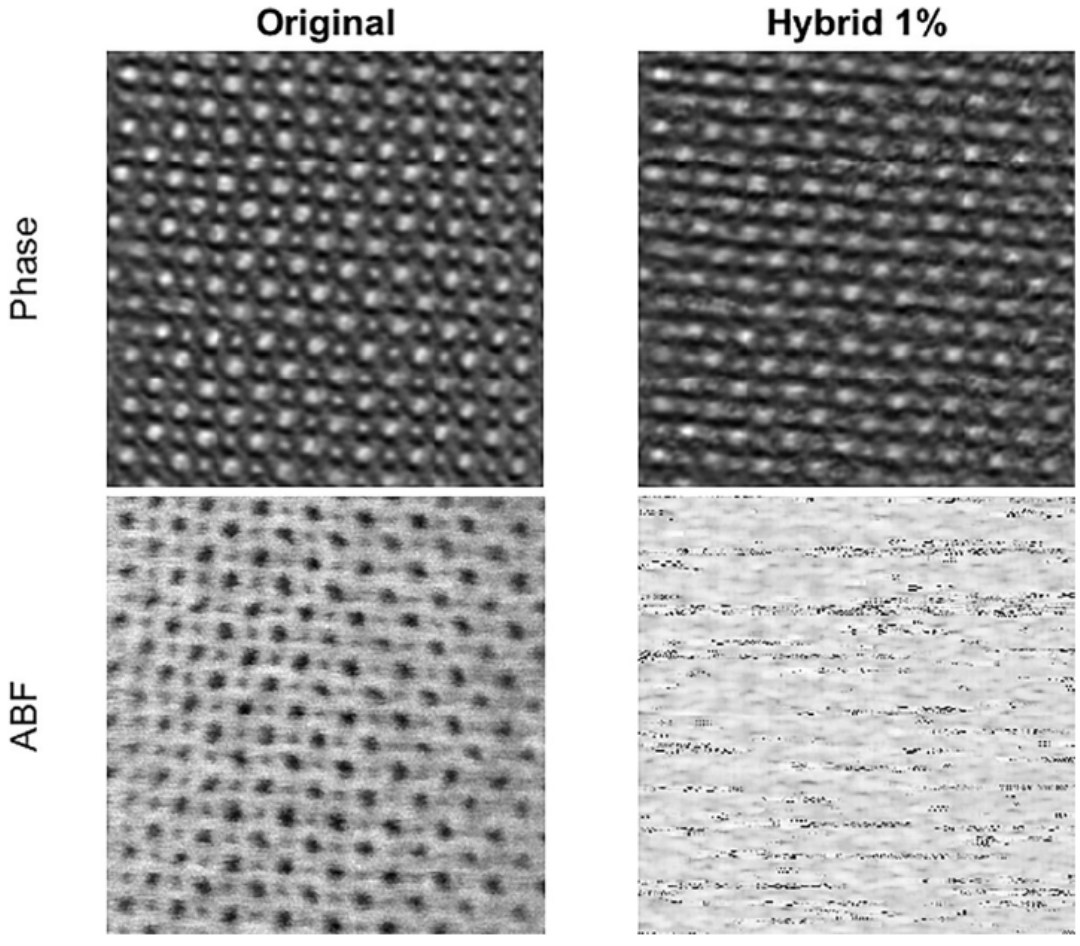

Random sampling

- 10% of original scan position **and**
- 10 % of original detector pixels

WDD Ptychography is still capable of Reconstructing the specimen.

A. Stevens et. al., Subsampled STEM-ptychography Appl. Phys. Lett. 113, 033104 (2018); https://doi.org/10.1063/1.5040496

Non-periodic specimen

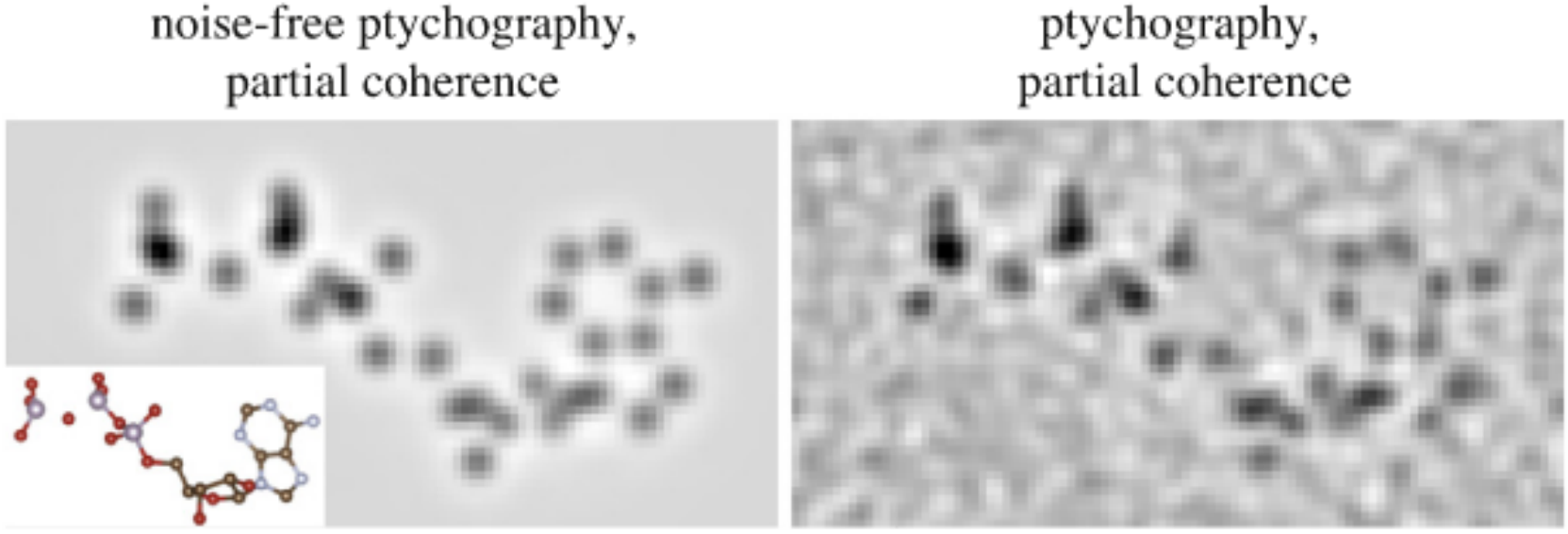

Phase contrast imaging of simulated data of an adenosine triphosphate (ATP) molecule at a dose of 20,000 e^- / Å^2. The model structure at the corner shows P in pink, O in red, N in light blue and C in brown. The reconstruction is made using SSB method.

Timothy J.Pennycook, High dose efficiency atomic resolution imaging via electron ptychography,Ultramicroscopy, 196, 2019

Dose Efficiency

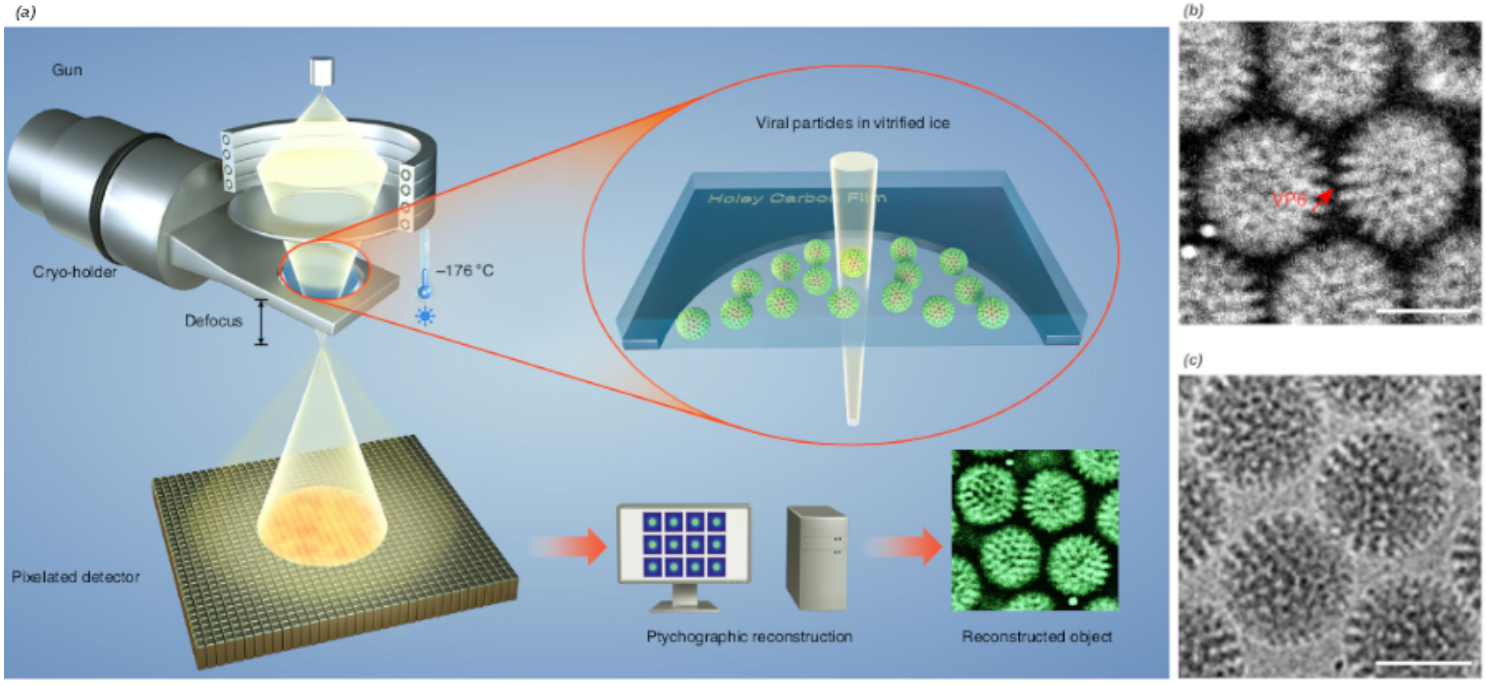

Reconstruction of frozen-hydrated specimen of rotavirus double-layered particles using ePIE shows extreamly high contrast. (a) A schematic of the setup and the reconstruction method. (b) phase image at a dose of 22.8 e^- / Å^2. (c)phase image at a dose of 35 e^- / Å^2. The scale bar is 50 nm.

Liqi Zhou, Low-dose phase retrieval of biological specimens using cryo-electron ptychography, Nature communications,2020

Simultaneous 4D data acquisition and ADF imaging

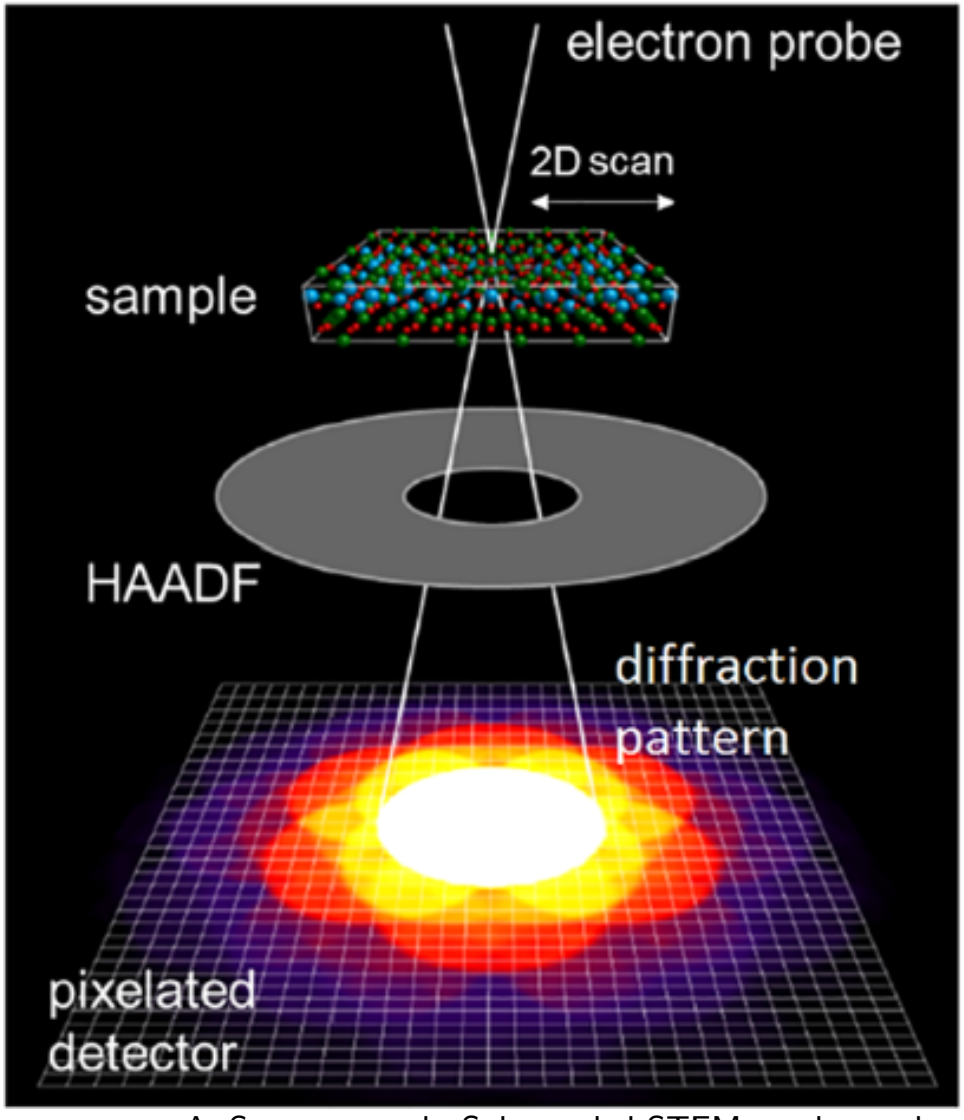

- scan speed 10^6 position per second
- recording time $\sim 10^3$ frame per second (fps)

A. Stevens et. al., Subsampled STEM-ptychography Appl. Phys. Lett. 113, 033104 (2018); https://doi.org/10.1063/1.5040496

Simultaneous 4D data acquisition and ADF imaging

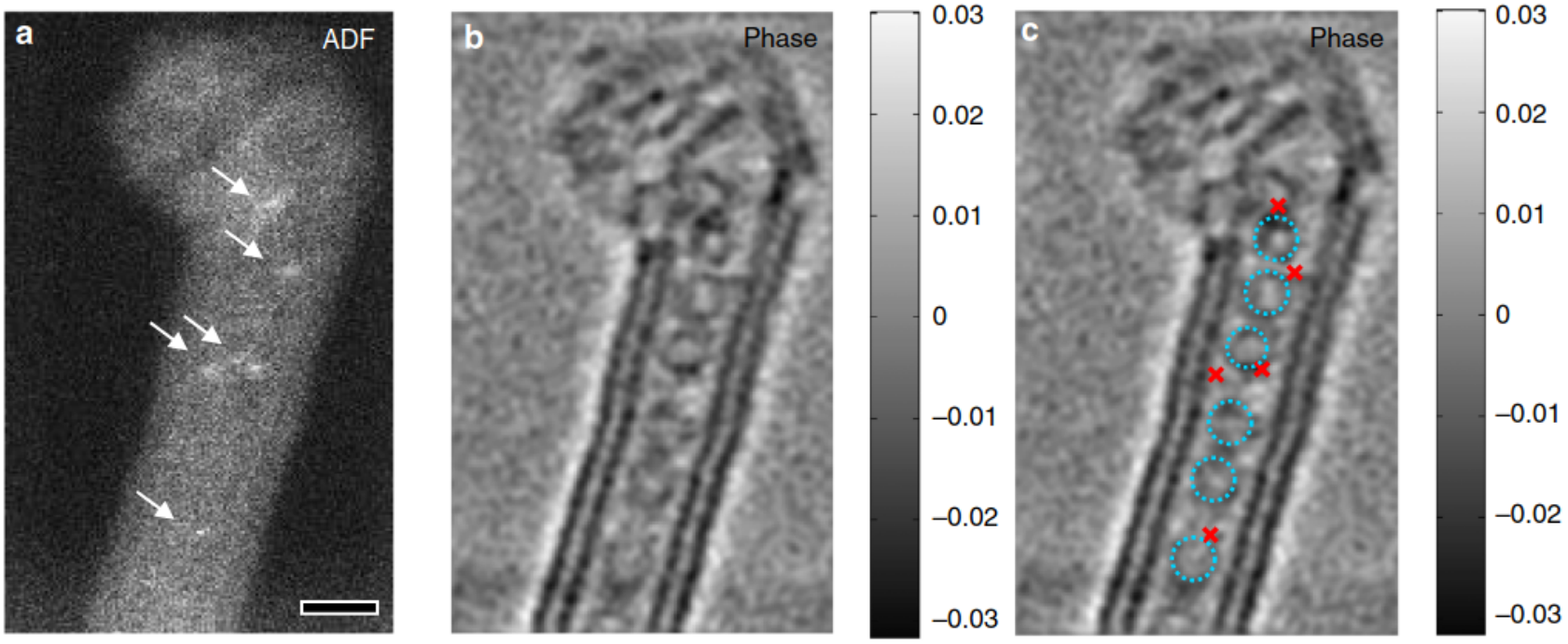

Characterization of Double-wall complex carbon nanotube (CNT) peapod. (a) Z-contrast ADF image. The arrows indicate the location of the single iodine atoms. (b) The phase image reconstructed using WDD method. (c) Full characterization is made by combining both methods.

H. Yang et. al. Simultaneous atomic-resolution electron ptychography and z-contrast imaging of light and heavy elements in complex nanostructures.Nature Commun, 7(12532

MoS2 structure

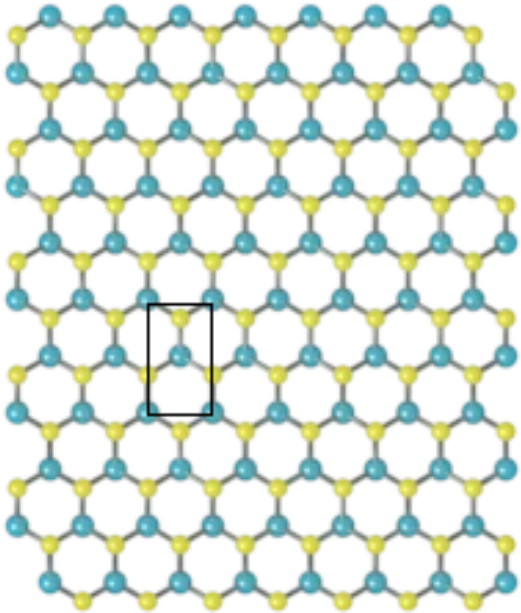

ossila.com, visited August 2020

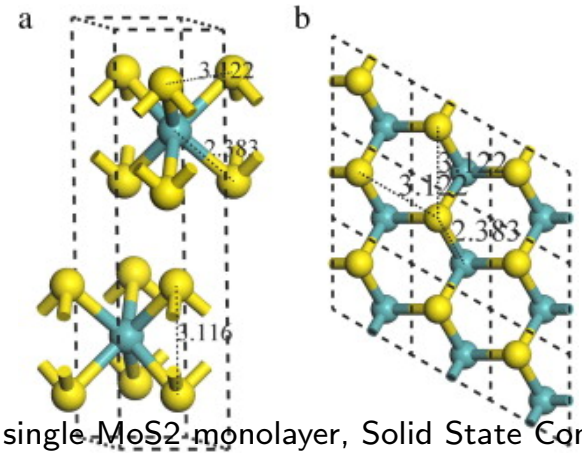

Eugene S. Kadantseva, Pawel Hawrylak, Electronic structure of a single MoS2 monolayer, Solid State Comm. 2012

Conventional STEM images

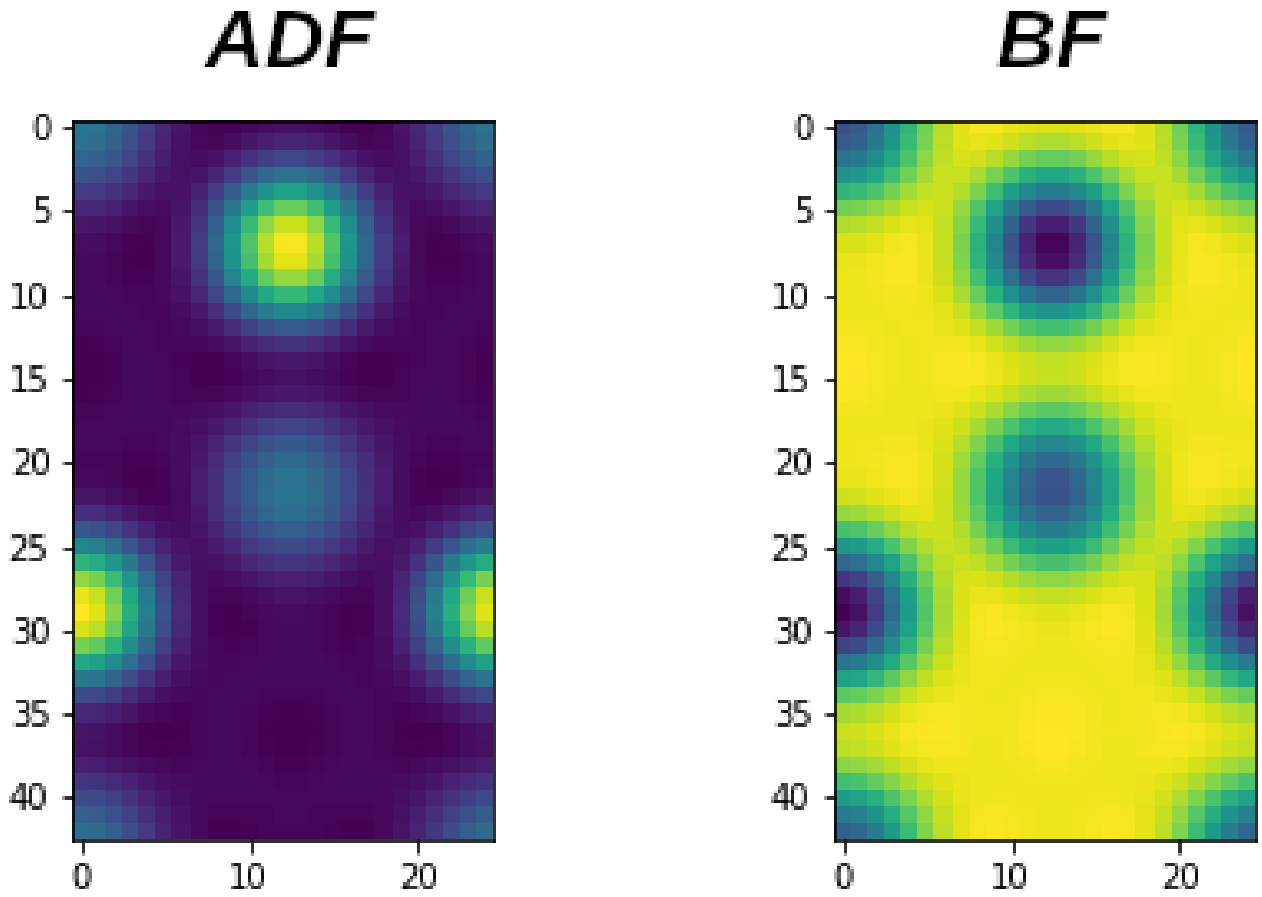

Annular dark field image (left) and bright field image (right) of the MoS2 mololayer. The images are constructed from the 4D data set using virtual detectors. The ADF image shows z-contrast. The image width is 316 pm.

Sigle Side-band Ptychography

The shorter version of WDD which makes use of the weak phase object approximation and applicable to thin specimens; the single side-band method SSB was applied to simulated monolayer MoS2. The image-width is 316 pm.

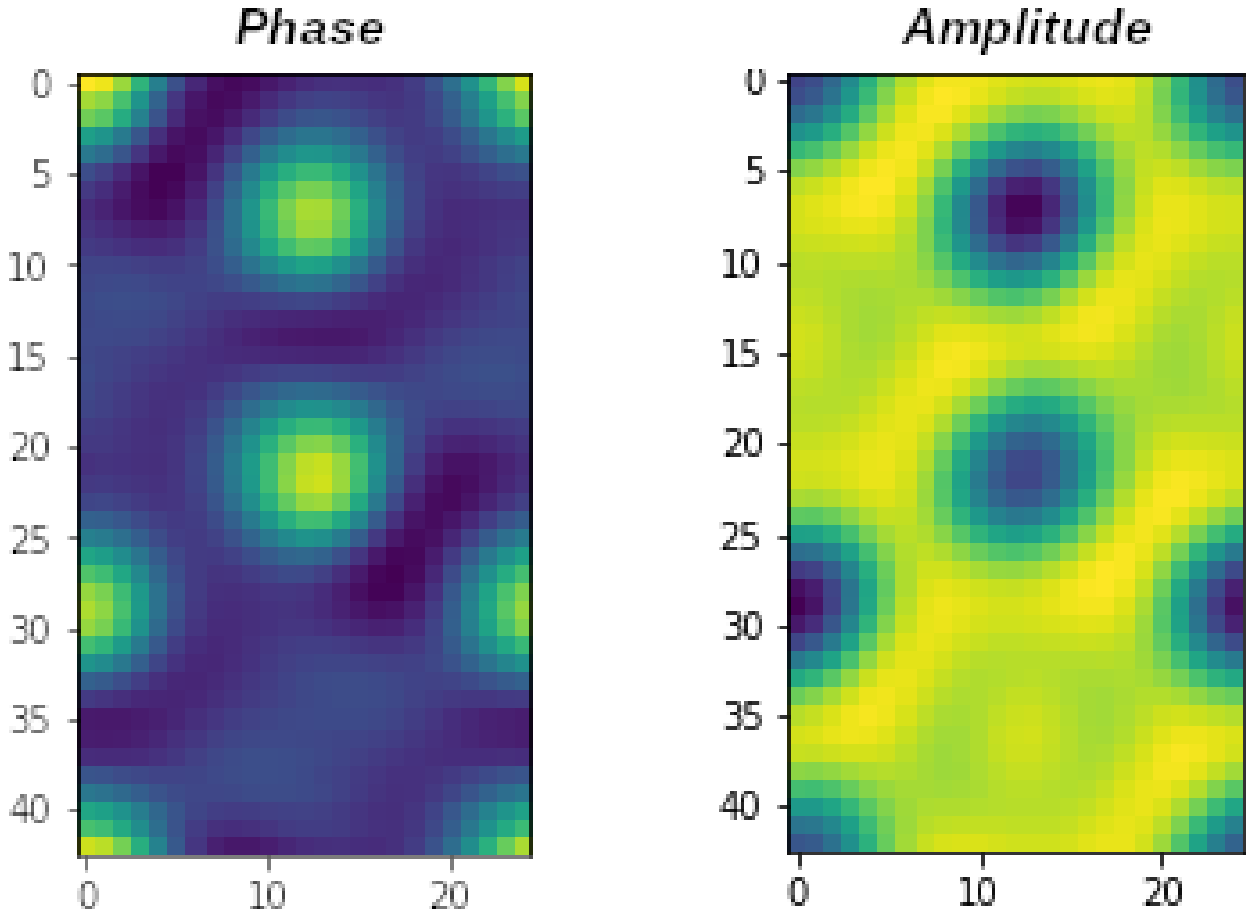

Figure: Phase and amplitude images of monolayer MoS2 using single

ADF images of gold specimen

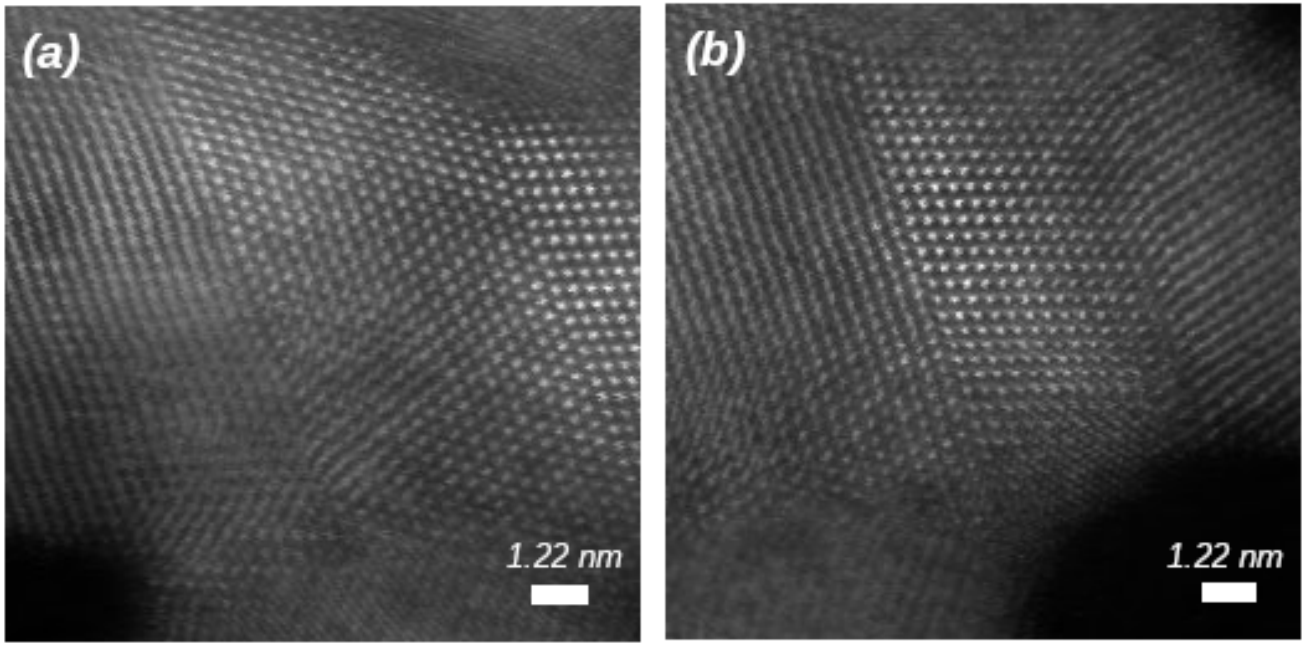

Figure: ADF images of very thin (< 5 nm) characterizing gold grid usually used for the FEI TITAN 30-800 STEM aberration correction. (a) Optimal image with aberrations appropriately corrected. (b) Aberrated image.

The images above was obtained on a laboratory session with H. L. Robert at The Ernst Ruska-Centre for Microscopy and Spectroscopy with Electrons on July 2020. They are obtained using Annular Dark Field detector.

Abberation measurement with ePIE

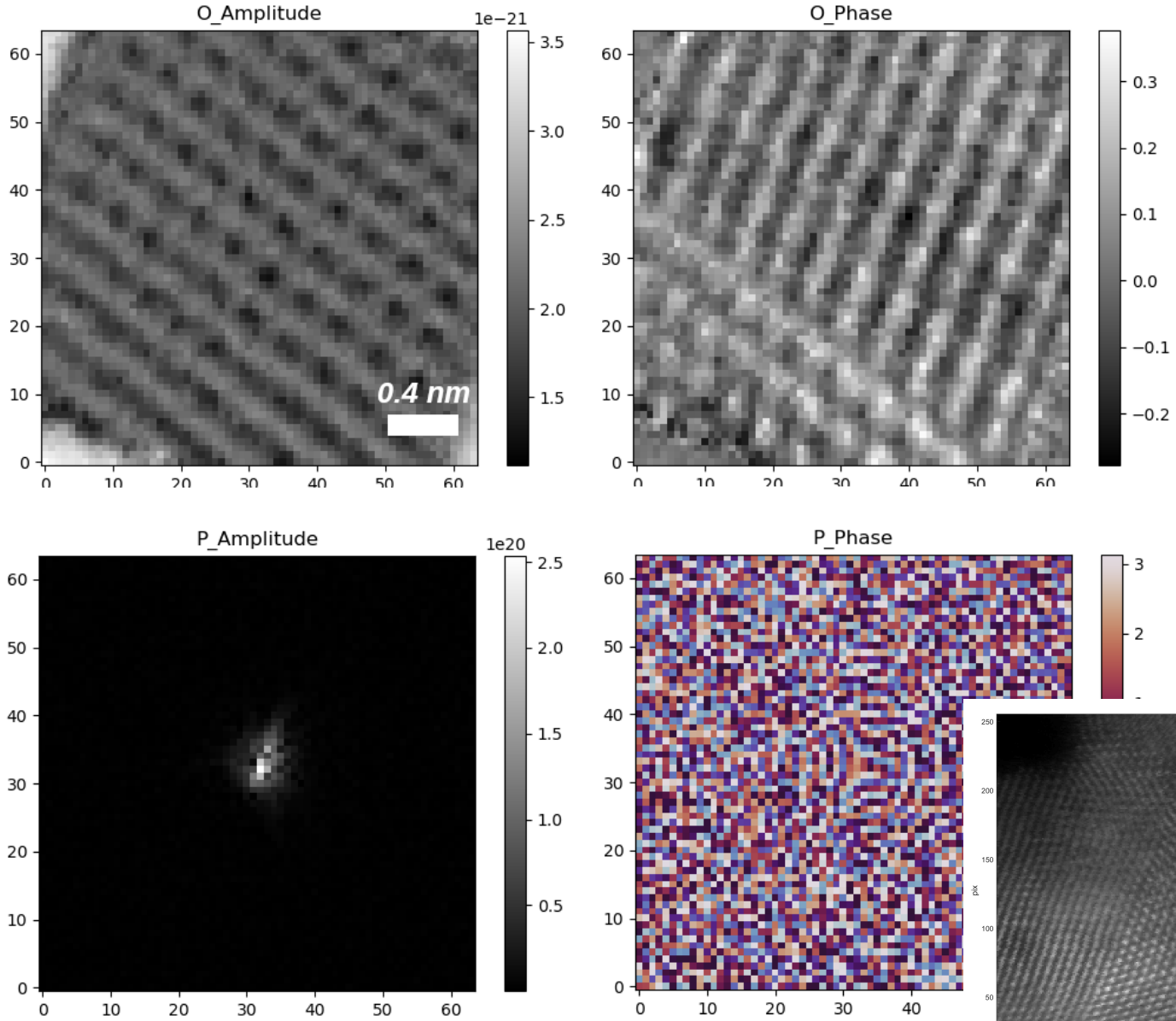

A. Strauch, moreSTEM ePIE reconstruction, 2020

Abberation measurement with ePIE

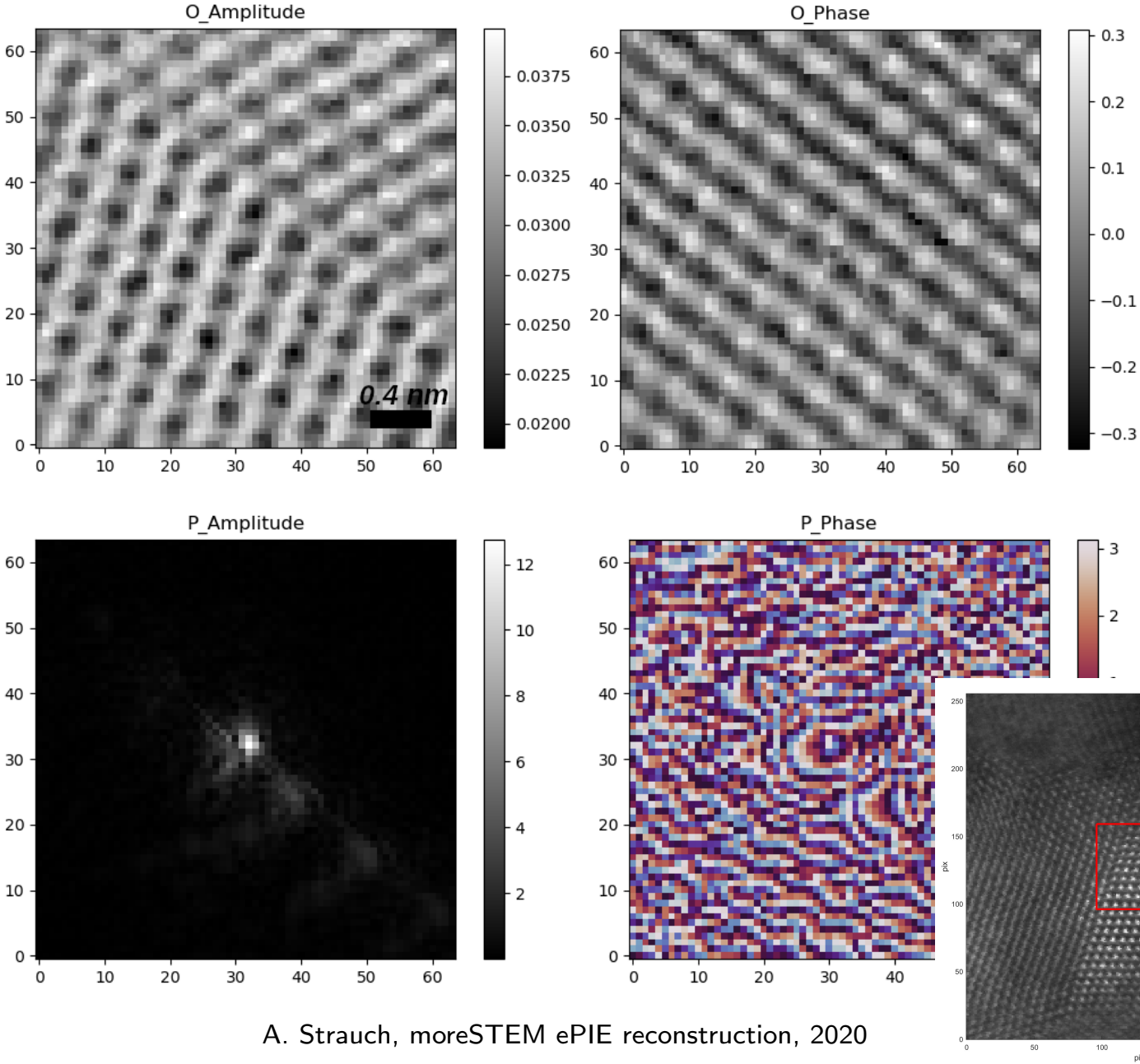

A. Strauch, moreSTEM ePIE reconstruction, 2020

Unit cell extraction from crystalline images

Crystals from a mathematical point of view

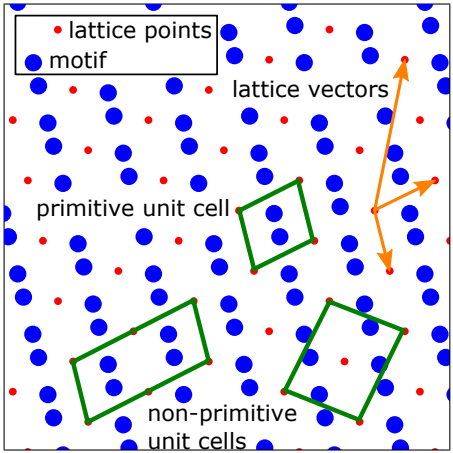

- crystals are defined through symmetry

  unit cell $U = \{\vec{v}_1, \ldots, \vec{v}_d\} \subset \mathbb{R}^d$

  motif $M = \{(\vec{m}_1, c_1), \ldots, (\vec{m}_n, c_n)\}$

Crystals from a mathematical point of view

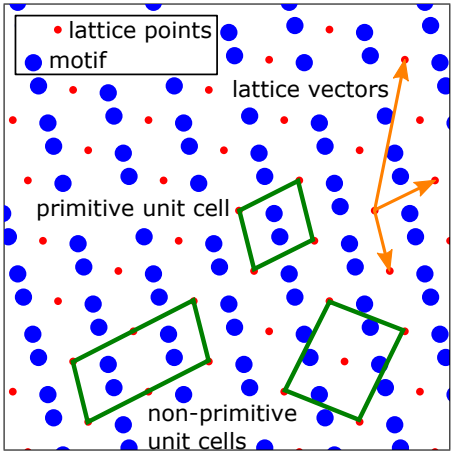

- crystals are defined through symmetry

  unit cell $U = \{\vec{v}_1, \ldots, \vec{v}_d\} \subset \mathbb{R}^d$

  motif $M = \{(\vec{m}_1, c_1), \ldots, (\vec{m}_n, c_n)\}$

$\rightarrow \mathscr{C}(U, M) = \left\{ \left(\vec{m}_j + \sum_{i=1}^{d} z_i \vec{v}_i, c_j \right) \,\middle|\, z_i \in \mathbb{Z} \right\}$

Crystals from a mathematical point of view

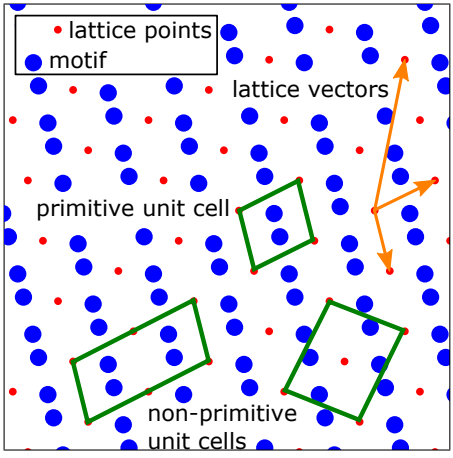

- crystals are defined through symmetry

  unit cell $U = \{\vec{v}_1, \ldots, \vec{v}_d\} \subset \mathbb{R}^d$

  motif $M = \{(\vec{m}_1, c_1), \ldots, (\vec{m}_n, c_n)\}$

$\rightarrow \mathscr{C}(U, M) = \left\{ \left(\vec{m}_j + \sum_{i=1}^{d} z_i \vec{v}_i, c_j \right) \,\middle|\, z_i \in \mathbb{Z} \right\}$

- *primitive* unit cells have minimal motif size

Crystals from a mathematical point of view

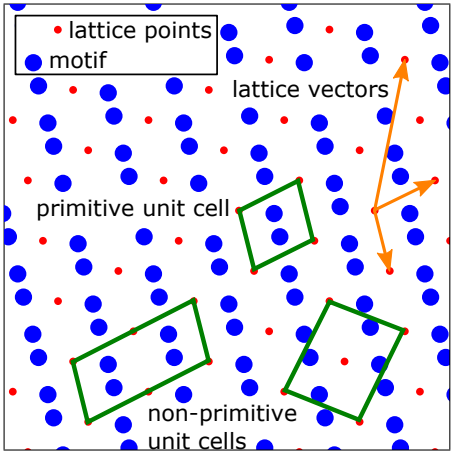

- crystals are defined through symmetry

  unit cell $U = \{\vec{v}_1, \ldots, \vec{v}_d\} \subset \mathbb{R}^d$

  motif $M = \{(\vec{m}_1, c_1), \ldots, (\vec{m}_n, c_n)\}$

$\rightarrow \mathscr{C}(U, M) = \left\{ \left(\vec{m}_j + \sum_{i=1}^{d} z_i \vec{v}_i, c_j \right) \,\middle|\, z_i \in \mathbb{Z} \right\}$

- *primitive* unit cells have minimal motif size
- crystal lattice generated by primitive unit cells
- lattice vector connects crystal lattice points

Challenges: noise, image distortions, crystal defects

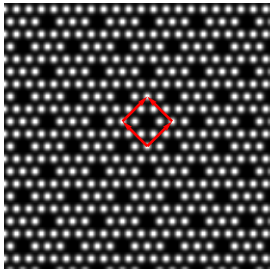

- Electron microscopy: projection $\rightarrow$ 2D image
- Image periodic along lattice vectors

Challenges: noise, image distortions, crystal defects

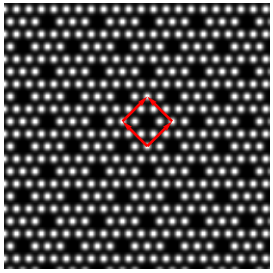

- Electron microscopy: projection $\rightarrow$ 2D image
- Image periodic along lattice vectors

$$E(\vec{v}_1, \vec{v}_2) = \sum_{(z_1,z_2)\in\mathcal{Z}} \int (f(x) - f(x + z_1\vec{v}_1 + z_2\vec{v}_2))^2 \, \mathrm{d}x$$

$$\mathcal{Z} = \{(1,0),(0,1),(1,1)\}$$

- Lattice vectors are roots of $E(\vec{v}_1, \vec{v}_2)$
- Shortest non-parallel root is primitive unit cell

$$(\vec{v}_1, \vec{v}_2) \in \underset{(\vec{u}_1,\vec{u}_2)\in\{E=0\}\cap\{\vec{u}_1\times\vec{u}_2\neq 0\}}{\arg\min} |\vec{u}_1| + |\vec{u}_2|$$

Challenges: noise, image distortions, crystal defects

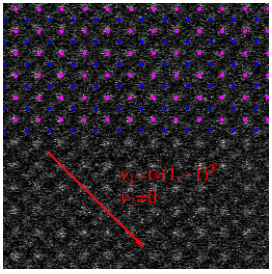

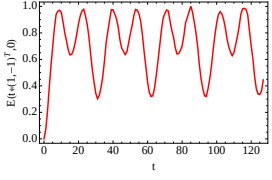

- Electron microscopy: projection $\rightarrow$ 2D image
- Image periodic along lattice vectors

$$E(\vec{v}_1, \vec{v}_2) = \sum_{(z_1,z_2)\in\mathcal{Z}} \int (f(x) - f(x + z_1\vec{v}_1 + z_2\vec{v}_2))^2 \, \mathrm{d}x$$

$$\mathcal{Z} = \{(1,0), (0,1), (1,1)\}$$

- Lattice vectors are roots of $E(\vec{v}_1, \vec{v}_2)$
- Shortest non-parallel root is primitive unit cell

$$(\vec{v}_1, \vec{v}_2) \in \underset{(\vec{u}_1,\vec{u}_2)\in\{E=0\}\cap\{\vec{u}_1\times\vec{u}_2\neq 0\}}{\arg\min} |\vec{u}_1| + |\vec{u}_2|$$

- In practice $E(v_1, v_2) = 0$ only for $v_1, v_2 = 0$
- Local minima $\nabla E(v_1, v_2) = 0$ ambiguous

$\rightarrow$ finding *primitive* unit cells non-trivial

Real-space analysis of lattice vector angles [Sang, LeBeau '14]

Three step procedure:

1. Lattice vector **angles**
2. Fundamental **periods**
3. Iterative refinement

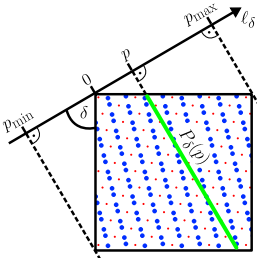

- project image onto lines ℓ_δ with angle δ

$\rightarrow$ average projected intensity:

$$A_\delta(p) = \int_{P_\delta(p)} f \, \mathrm{d}x \text{ for } |P_\delta(p)| > 0 \text{ and zero else}$$

- $\delta + \frac{\pi}{2}$ angle of lattice vector $\Rightarrow$ periodic signal

Real-space analysis of lattice vector angles [Sang, LeBeau '14]

Three step procedure:

1. Lattice vector **angles**
2. Fundamental **periods**
3. Iterative refinement

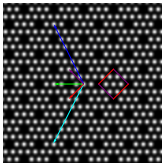

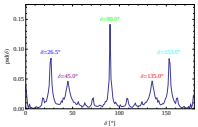

- project image onto lines ℓ_δ with angle δ

$\rightarrow$ average projected intensity:

$$A_\delta(p) = \int_{P_\delta(p)} f \, \mathrm{d}x \text{ for } |P_\delta(p)| > 0 \text{ and zero else}$$

- $\delta + \frac{\pi}{2}$ angle of lattice vector $\Rightarrow$ periodic signal

$\rightarrow$ maximize variance of A_δ against δ

$$\mathrm{psd}^2(\delta) = \int_{p_{\min}}^{p_{\max}} \left(A_\delta(p) - \mu_\delta\right)^2 \, \mathrm{d}p$$

$$\mu_\delta = \int_{p_{\min}}^{p_{\max}} A_\delta(p) \, \mathrm{d}p$$

- peaks of psd $=$ lattice vector angles

Real-space analysis of fundamental periods [Mevenkamp, Berkels '15]

Three step procedure:

1. Lattice vector **angles**
2. Fundamental **periods**
3. Iterative refinement

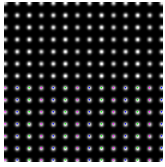

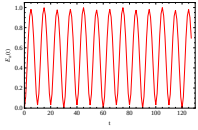

- assume lattice vector angle α is given
- how to find the desired local minimum?

$$E_\alpha(t) = \left(f(x + t\vec{e}_\alpha) - f(x)\right)^2 \, \mathrm{d}x \text{ with } e_\alpha = \begin{pmatrix} \cos\alpha \\ \sin\alpha \end{pmatrix}$$

Real-space analysis of fundamental periods [Mevenkamp, Berkels '15]

Three step procedure:

1. Lattice vector **angles**
2. Fundamental **periods**
3. Iterative refinement

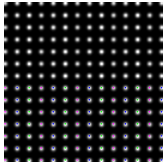

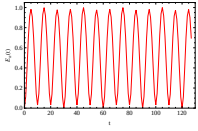

- assume lattice vector angle α is given
- how to find the desired local minimum?

$$E_\alpha(t) = (f(x + t\vec{e}_\alpha) - f(x))^2 \, \mathrm{d}x \text{ with } e_\alpha = \begin{pmatrix} \cos\alpha \\ \sin\alpha \end{pmatrix}$$

1. cluster local minimizers of $E_\alpha(t)$
2. select cluster with smallest energy
3. select element with smallest period t

Real-space analysis of fundamental periods [Mevenkamp, Berkels '15]

Three step procedure:

1. Lattice vector **angles**
2. Fundamental **periods**
3. Iterative refinement

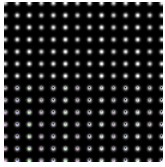

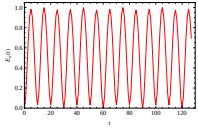

- assume lattice vector angle α is given
- how to find the desired local minimum?

$$E_\alpha(t) = \left(f(x + t\vec{e_\alpha}) - f(x)\right)^2 \, \mathrm{d}x \text{ with } e_\alpha = \begin{pmatrix} \cos\alpha \\ \sin\alpha \end{pmatrix}$$

1. cluster local minimizers of $E_\alpha(t)$
2. select cluster with smallest energy
3. select element with smallest period t

Note

- the correct number of clusters is crucial
- robust automatic determination possible
- involves likelihoods of multi-variance cluster models induced by the Akaike information criterion (AIC)

Final estimate via non-linear regression [Mevenkamp, Berkels '15]

Three step procedure:

1. Lattice vector **angles**
2. Fundamental **periods**
3. Iterative refinement

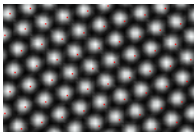

- set of candidate lattice vectors

$$V^* = \{T_{\alpha_1} e_{\alpha_1}, \dots, T_{\alpha_n} e_{\alpha_n}\}$$

$\rightarrow$ select estimate primitive unit cell

$$v_1 = \operatorname*{arg\,min}_{u \in V^*} |u|, \quad v_2 = \operatorname*{arg\,min}_{u \in V^* \setminus \{v_1\}} |u|$$

Final estimate via non-linear regression [Mevenkamp, Berkels '15]

Three step procedure:

1. Lattice vector **angles**
2. Fundamental **periods**
3. Iterative refinement

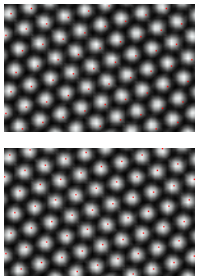

- set of candidate lattice vectors

$$V^* = \{T_{\alpha_1} e_{\alpha_1}, \dots, T_{\alpha_n} e_{\alpha_n}\}$$

$\rightarrow$ select estimate primitive unit cell

$$v_1 = \operatorname*{arg\,min}_{u \in V^*} |u|, \quad v_2 = \operatorname*{arg\,min}_{u \in V^* \setminus \{v_1\}} |u|$$

- in discrete setting energy sum of squares

$$\begin{aligned}\hat{E}(v_1, v_2) &= \sum_{(z_1,z_2)\in\mathcal{Z}} \sum_i (f(x_i) - f(x_i + z_1 v_1 + z_2 v_2))^2 \\ &= \|F(v)\|_2^2 \qquad (\mathcal{Z} = \{(1,0),(0,1),(1,1)\})\end{aligned}$$

$\rightarrow$ non-linear regression (e.g. Gauß-Newton)

$$v^{n+1} = v^n + \operatorname*{arg\,min}_s \tfrac{1}{2}\|\nabla F(v^n)s + F(v^n)\|_2^2 \text{ with } v^0 = (v_1, v_2)$$

Results on experimental data

"17 1316 11.0 Mx 9.02 nm HAADF-DF4-DF2 D DCFI(HAADF)" from B01

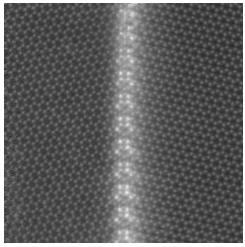

Original Image

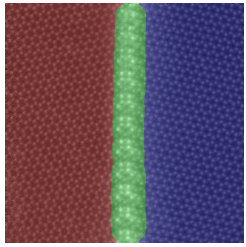

Segmentation

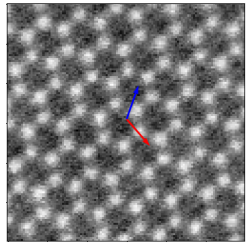

Left grain's unit cell

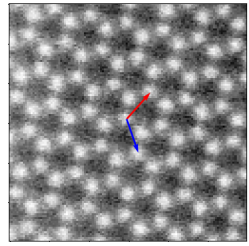

Right grain's unit cell

The computed angle between the neighboring grains is 22.3, which is in good agreement with the MD simulations of A02.

Results on experimental data

"7 11.0 Mx 9.02 nm HAADF-DF4-DF2 D DCFI(HAADF)" from B01

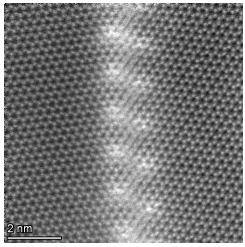

Original Image

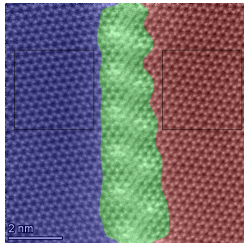

Segmentation

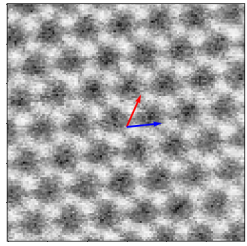

Left grain's unit cell

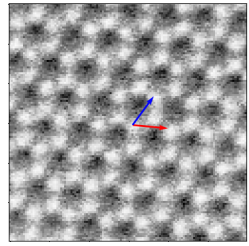

Right grain's unit cell

The computed angle between the neighboring grains is 12.6, which is in good agreement with the MD simulations of A02.

Results on experimental data

"1 11.0 Mx 9.02 nm HAADF-DF4-DF2 D DCFI(HAADF)" from B01

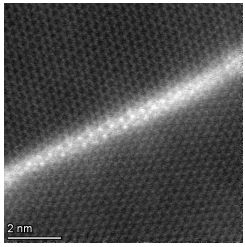

Original Image

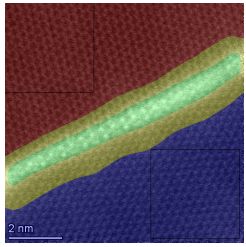

Segmentation

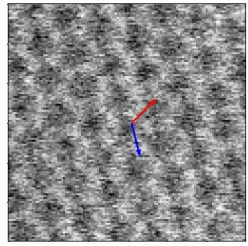

Left grain's unit cell

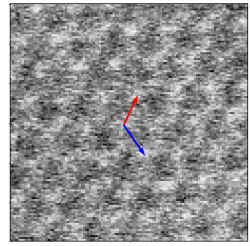

Right grain's unit cell

The computed angle between the neighboring grains is 20.8, which is in good agreement with the MD simulations of A02.

Results on experimental data

Al_2Ca-Mg data provided by B01

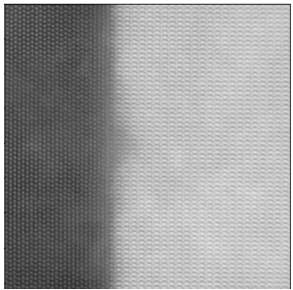

Original Image

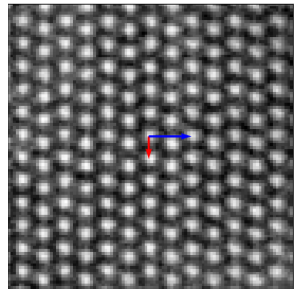

Left grain's unit cell

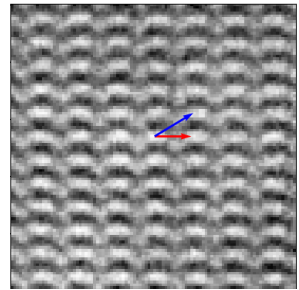

Right grain's unit cell

Results on experimental data

Al_2Ca-Mg data provided by B01

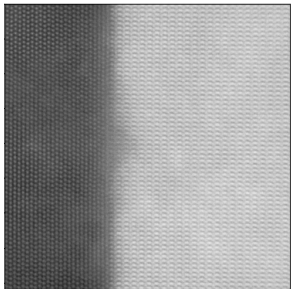

Original Image

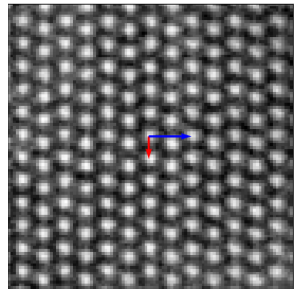

Left grain's unit cell

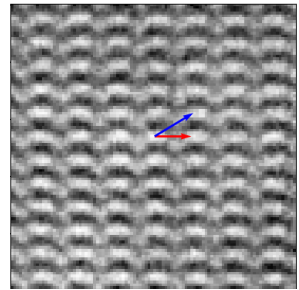

Right grain's unit cell

Next steps: Error bars, motif extraction.

Application on simulated data

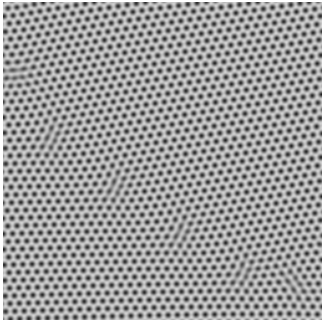

Original Image

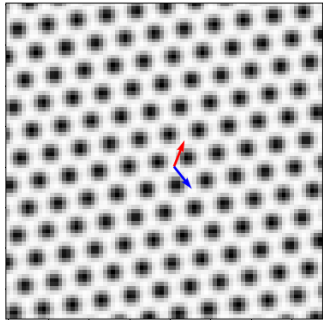

Unit cell vectors

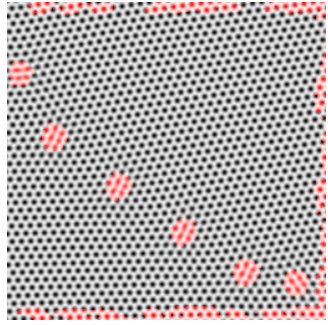

Defects

First the unit cell was determined. The unit cell vectors were then used to determine the lattice defects.

Acknowledgement

I would like to thank my supervisors for their patient guidance,
valuable advises and the kindness they treated me with.
I have been lucky to be closely mentored.

I thank both ICTP and ER-C for the period I spent in Jülich.

I would like to thank SFB 409476157 for their generous support fot
the Crystal analysis of high resolution image data project